Third-order optical intensity correlation measurements of pseudo-thermal light*

Chen Xi-Hao(陈希浩)[a], Wu Wei(吴 炜)[a], Meng Shao-Ying(孟少英)[a]†, and Li Ming-Fei(李明飞)[b]‡

[a] College of Physics, Liaoning University, Shenyang 110036, China
[b] Laboratory of Optical Physics, Institute of Physics, Chinese Academy of Sciences, Beijing 100190, China

(Received 15 January 2014; revised manuscript received 10 March 2014; published online 24 July 2014)

Third-order Hanbrury Brown–Twiss and double-slit interference experiments with a pseudo-thermal light are performed by recording intensities in single, double and triple optical paths, respectively. The experimental results verifies the theoretical prediction that the indispensable condition for achieving a interference pattern or ghost image in *N*th-order intensity correlation measurements is the synchronous detection of the same light field by each reference detector, no matter the intensities recorded in one, or two, or *N* optical paths. It is shown that, when the reference detectors are scanned in the opposite directions, the visibility and resolution of the third-order spatial correlation function of thermal light is much better than that scanned in the same direction, but it is no use for obtaining the *N*th-order interference pattern or ghost image in the thermal *N*th-order interference or ghost imaging.

Keywords: third-order intensity correlation, thermal double-slit interference, pseudo-thermal light

PACS: 07.05.Pj, 42.25.Hz, 42.25.Kb **DOI:** 10.1088/1674-1056/23/9/090701

1. Introduction

Since the first optical intensity correlation experiment with thermal light was performed by Hanbury Brown and Twiss (HBT) in 1956,[1,2] it has attracted great interest and been extensively studied. Decades later, in 1995, the first "ghost" interference (GI) experiment with two-photon entangled light[3] was performed, and then the spatial HBT-type experiments on second-order GI and ghost imaging with classical thermal light have aroused much more attention.[4–17] However, due to the low visibility in the second-order GI and ghost imaging, many recent reports on the intensity correlation effects[18–34] have been focused on the higher-order GI and ghost imaging.

So far, the higher-order GI and ghost imaging with thermal light has been widely analyzed both in theory[18,19,23–25,28–30,35,36] and in experiment.[20–22,26,27,31–34] The first multi-photon interference experiment with classical light was performed by Agafonov *et al.*,[20] who also proposed a high-order scheme to obtain improved visibility and signal-to-noise ratio for ghost imaging.[21] The first *N*th-order ($N \geq 2$) ghost imaging experiment in a lensless scheme was performed by recording only the intensities in two optical paths.[26] Recently, the first third-order thermal GI experiment was performed by recording the intensities in three optical paths and verified that the enhanced visibility of the *N*th-order GI is a consequence of the contribution of *N*th-order intensity fluctuation correlations. Zeng's group utilized a periodic point source to perform a periodic diffraction correlation imaging experiment without a beam splitter[31] and later they gave a detailed quality analysis of ideal high-order thermal ghost imaging.[32] Shih's group investigated the high-order coherence of thermal light based on Glauber's quantum optical coherence[30] and then performed third-order HBT and ghost imaging experiments with thermal light in the photon counting regime.[33,34] However, most of these thermal high-order experiments have been implemented by recording the intensities in optical paths by means of one or two detectors.

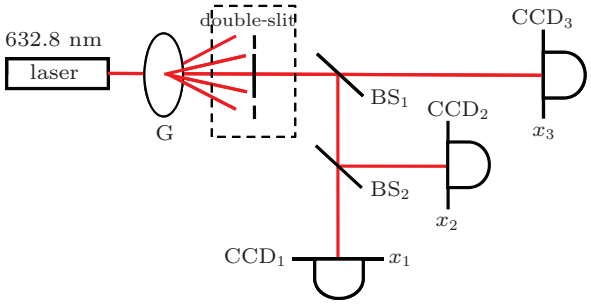


Fig. 1. (color online) Experimental setup for the third-order intensity correlation measurement with a pseudo-thermal light source. G: rotating ground glass plate; BS: beamsplitter; CCD_i ($i = 1,2,3$): CCD camera.

In this paper, we report the experimental demonstration of the third-order spatial intensity correlation measurements and double-slit interferences with pseudo-thermal light by recording the intensities in single, double and triple optical paths, respectively. The theoretical prediction in Ref. [18] that the

*Project supported by the National Natural Science Foundation of China (Grant Nos. 11204117 and 11005055), the China Postdoctoral Science Foundation of China (Grant No. 2013M540146), and the Education Department of Liaoning Province, China (Grant Nos. L2012001 and LJQ2011005).

†Corresponding author. E-mail: mengshaoying@163.com
‡Corresponding author. E-mail: mf_li@sina.cn

© 2014 Chinese Physical Society and IOP Publishing Ltd

necessary condition for achieving an Nth-order interference pattern or ghost image in Nth-order intensity correlation measurements is the synchronous detection of the same light field by reference detectors is proved experimentally. It is shown that though the visibility and resolution in the third-order intensity correlation function can be dramatically enhanced by scanning the reference detectors in the opposite directions, it is useless for obtaining the Nth-order interference pattern or ghost image in the higher-order thermal interference or ghost imaging experiments.

2. Theory

In the high-intensity limit, the normalized third-order correlation function in the detection plane can be given by[37]

$$g^{(3)}(x_1,x_2,x_3)=\frac{\langle I_1(x_1)I_2(x_2)I_3(x_3)\rangle}{\langle I_1(x_1)\rangle\langle I_2(x_2)\rangle\langle I_3(x_3)\rangle}, \tag{1}$$

where $I_j(x_j)$ $(j=1,2,3)$ is the instantaneous intensity at the transverse position x_j in this plane and $\langle\cdots\rangle$ stands for ensemble averaging. Here for simplicity but without loss of generality, we assume that the transverse position x_j mentioned above is one-dimensional and also in the experimental data processing below.

According to Ref. [18], we can rewrite this normalized correlation function for thermal light in terms of the intensity fluctuation correlation

$$\begin{aligned} g^{(3)}(x_1,x_2,x_3) &= 1+\Delta g^{(2)}_{12}(x_1,x_2)+\Delta g^{(2)}_{23}(x_2,x_3) \\ &\quad +\Delta g^{(2)}_{13}(x_1,x_3)+\Delta g^{(3)}_{123}(x_1,x_2,x_3), \end{aligned} \tag{2}$$

where

$$\Delta g^{(3)}_{123}(x_1,x_2,x_3)=\frac{\langle \Delta I_1(x_1)\Delta I_2(x_2)\Delta I_3(x_3)\rangle}{\langle I_1(x_1)\rangle\langle I_2(x_2)\rangle\langle I_3(x_3)\rangle}, \tag{3}$$

and

$$\begin{aligned} &\Delta g^{(2)}_{ij}(x_i,x_j)=\frac{\langle \Delta I_i(x_i)\Delta I_j(x_j)\rangle}{\langle I_i(x_i)\rangle\langle I_j(x_j)\rangle}, \\ &(i\neq j,\quad i=1,2,\quad j=2,3), \end{aligned} \tag{4}$$

in which $\Delta g^{(n)}$ $(n=2,\ 3)$ is the optical intensity fluctuation correlation functions of thermal light source and the instantaneous intensity fluctuation $\Delta I(x)$ is equal to the difference between the instantaneous intensity of $I(x)$ and its average of $\langle I(x)\rangle$, namely, $\Delta I(x)=I(x)-\langle I(x)\rangle$.

3. Experiments and results

An outline of the experimental setup for the third-order intensity correlation measurement of pseudo-thermal light is shown in Fig. 1. An He–Ne laser beam with a wavelength of $\lambda=632.8$ nm and a beam diameter of D=3.5 mm is projected onto a rotating ground-glass plate G to produce a pseudo-thermal light. The scattered beam is first separated by a 50:50 non-polarizing beam splitter (BS_1) into two beams. The reflected beam passes through a second 50:50 non-polarizing BS_2, so the pseudo-thermal beam is divided into altogether three beams, which are detected by the charged-coupled-device (CCD) cameras CCD_1, CCD_2, and CCD_3 (Imaging Source DMK 41BU02), respectively. The CCDs are operated in the trigger mode and synchronized by the same trigger pulse. The data are acquired with an exposure time (0.6 ms) much shorter than the correlation time of the light source, which is on the order of 0.2 s, and saved through a USB cable to a computer. All the experimental results were obtained by averaging about 40000 exposure frames. For convenience, we name the light beam and CCD_1 in path 1 as the test beam and test detector, respectively, while the other two beams and CCDs are called the reference beams and reference detectors in the whole paper.

We first performed the third-order spatial HBT experiment with the pseudo-thermal light. The distances between the pseudo-thermal light source and the three CCDs are all 346 mm. According to Eq. (1), we calculated the third-order intensity correlation functions with the data acquired respectively from the three CCDs, from CCD_1 and CCD_2, from CCD_1 and CCD_3 and from CCD_1 itself (auto-correlation HBT scheme), where we chose the CCD_1 as the point detector. The corresponding normalized third-order intensity correlation function are expressed as $g^{(3)}_{123}(x_1,x_2,x_3)$, $g^{(3)}_{122}(x_1,x_2,x_3)$, $g^{(3)}_{133}(x_1,x_2,x_3)$, and $g^{(3)}_{111}(x_1,x_2,x_3)$. The experimental results of the third-order intensity correlation function are shown in Figs. 2(a)–2(d), respectively, in which the black dot cross curves are obtained by scanning the two reference detectors synchronously, namely, keeping $x_3=x_2$ with the position of CCD_1 fixed at $x_1=0$. When the two reference detectors are scanned in opposite directions, namely, $x_3=-x_2$ with $x_1=0$, we obtain the red dot cross curves. It can be seen in Fig. 2 that the four black (and red dot) cross curves are almost the same, i.e., $g^{(3)}_{123}(x_1,x_2,x_3)=g^{(3)}_{122}(x_1,x_2,x_3)=g^{(3)}_{133}(x_1,x_2,x_3)=g^{(3)}_{111}(x_1,x_2,x_3)$. That is to say, no matter the intensities are recorded with single, double or triple detectors, the interference fringes of the third-order correlation functions are almost the same. This is a hard proof of the equivalence of the one or two and even N detectors scheme in the thermal Nth-order interference or ghost imaging.[17,22,28] Moreover, the profiles in Fig. 2 also reflect the fact that the correlation length determines the pattern resolution. In general, the resolution is expressed as the full width at half maximum (FWHM) of the curves, and the narrower the FWHM is, the better the resolution is. One can easily see from Fig. 2 that the FWHM of the red ones is narrower than that of the black curves, for example, in Fig. 2(a), the measured FWHMs are

about 0.10 mm for the red curve and 0.14 mm for the black one. Therefore, the visibility and resolution of the red curves in Fig. 2 are much better than those of the black ones. It means that the visibility and resolution of the third-order spatial HBT-type correlation function of thermal light can be dramatically enhanced by scanning the reference detectors in the opposite direction compared with the synchronous scan case, as has been predicted theoretically and observed experimentally in Ref. [34]. This enhancement of visibility is due to the contribution of the cross-correlation $\Delta g^{(3)}_{23}(x_2,x_3)$ from the beam 2 and beam 3, while that of resolution has to include the extra contribution of the third-order intensity fluctuation correlation $\Delta g^{(3)}_{123}(x_1,x_2,x_3)$.

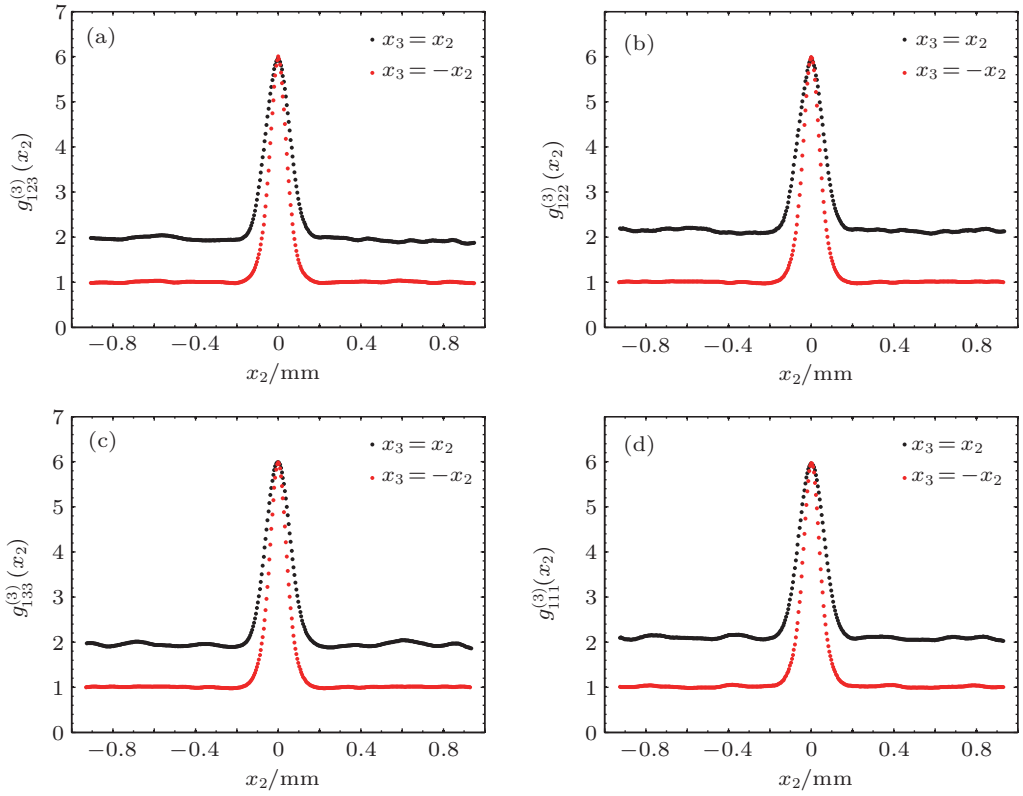


Fig. 2. (color online) Experimental results of third-order spatial HBT-type measurements. Black dot cross curves: the third-order correlation functions of $g^{(3)}(0,x_2,x_2)$; red dot cross curves: the third-order correlation functions of $g^{(3)}(0,x_2,-x_2)$. (a) $g^{(3)}_{123}$ obtained by the data from the three CCDs; (b) $g^{(3)}_{122}$ from CCD_1 and CCD_2; (c) $g^{(3)}_{133}$ from CCD_1 and CCD_3; and (d) $g^{(3)}_{111}$ from CCD_1.

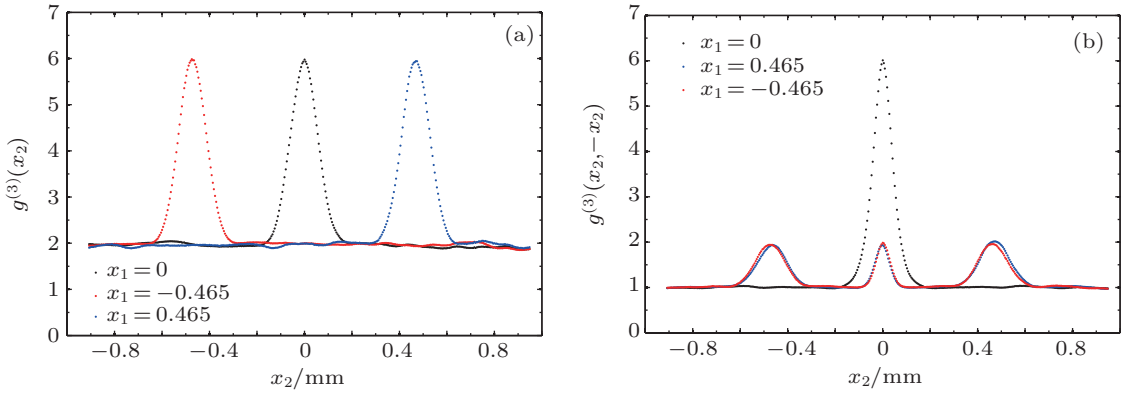


Fig. 3. (color online) Third-order HBT measurements of $g^{(3)}(x_2)$. (a) $g^{(3)}(x_2)$ for different x_1 when $x_3 = x_2$; (b) $g^{(3)}(x_2)$ for different x_1 when $x_3 = -x_2$.

However, the above enhancement of the visibility and resolution does no exist for the thermal higher-order interference and ghost imaging. This conclusion can be verified in our experiment by Fig. 3, where the third-order correlation function $g^{(3)}$ against x_2 for different x_1 are shown when the two reference detectors are scanned synchronously and in the opposite direction, respectively. It is shown that the third-order correlation function for different x_1 appears anywhere in the trans-

verse detection plane when $x_3 = x_2$, while it only exists near $x_1 = 0$ when $x_3 = -x_2$. Therefore, the third-order interference and ghosting imaging cannot be achieved when the two detectors are scanned in the opposite directions, since the third-order correlation does not always exist for any value of x_1. For the more higher-order interference and ghosting image, we can obtain the same conclusion. This implies that the necessary condition for achieving an Nth-order interference pattern or ghost image in Nth-order intensity correlation measurements is the synchronous detection of the same light field by each reference detector, as predicted theoretically in Ref. [18].

Then a double slit with a slit width of 200 μm and a separation of 400 μm is placed between G and BS_1, and the thermal third-order double-slit experiments were performed with the same three independent optical paths as those in the above HBT experiment. The distances between the double slit and three CCDs are 336 mm. According to Eq. (1), the third-order GI patterns are obtained by processing the data in the same way as the above HBT experiments and shown in Fig. 4. The black dot cross curves in Fig. 4 are the GI patterns obtained by scanning the two reference detectors synchronously, namely, keeping $x_3 = x_2$ with the position of CCD_1 fixed at $x_1 = 0$. While the red dot cross curves are obtained when the two reference detectors are scanned in the opposite direction, namely, $x_3 = -x_2$ with $x_1 = 0$. It is shown that the profiles of the red curves are distorted and are not the same as those of the black ones, where the distortion is due to the contribution of $\Delta g^{(3)}_{123}(x_1,x_2,x_3)$ and $\Delta g^{(2)}_{23}(x_2,x_3)$. In addition, although the visibility and resolution of the red curves are enhanced compared with the black ones, this improvement is not significant because the third-order GI patterns are no longer the same. For the case where $x_3 = -x_2$ and x_1 is far away from 0, like the above HBT experiment, it can be inferred that there may be no third-order correlation term, and the interference pattern is the superposition of two second-order terms. This implies that, when $x_3 = -x_2$ and x_1 is far away from 0, it is no longer the third-order correlation, much less the enhancement of the visibility and resolution. Therefore, to achieve the Nth-order interference pattern or ghost image in the Nth-order intensity correlation measurements, the synchronous detection of the same light field by different reference detectors is necessary, as has been theoretically predicted in Ref. [18]. This means that scanning the reference detectors in the opposite directions cannot be used to enhance the visibility and resolution of the thermal Nth-order interference pattern or ghost image.

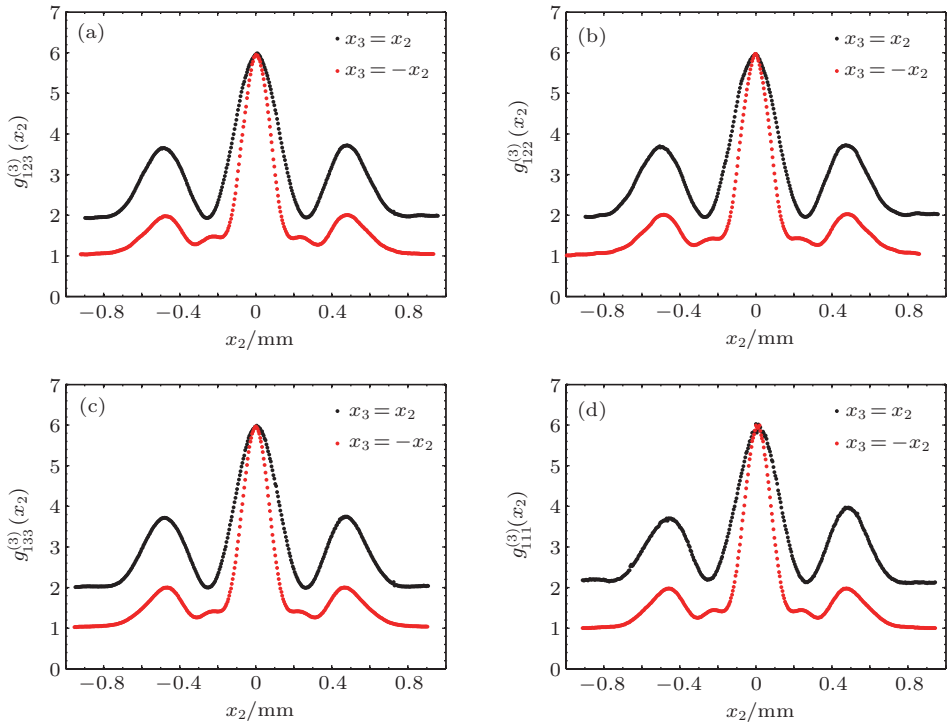


Fig. 4. (color online) Experimental results of the third-order double-slit interference with pseudo-thermal light. Black dot cross curves: the third-order double-slit interference of $g^{(3)}(0,x_2,x_2)$; red dot cross curves: the third-order double-slit interference of $g^{(3)}(0,x_2,-x_2)$. (a) $g^{(3)}_{123}$ obtained from the data from the three CCDs; (b) $g^{(3)}_{122}$ from CCD_1 and CCD_2; (c) $g^{(3)}_{133}$ from CCD_1 and CCD_3; (d) and $g^{(3)}_{111}$ from CCD_1.

In order to describe the role of each term in Eq. (2) and their influence on the above experimental results in detail, we plot their curves versus x_2 in two cases, i.e., $x_3 = x_2$ and $x_3 = -x_2$. The graphics with the data acquired from the three CCDs are shown in Fig. 5. For the case of $x_3 = x_2$, one can see obviously in Fig. 5(a) that there are three contribution terms ($\Delta g^{(2)}_{12}(x_1,x_2)$, $\Delta g^{(2)}_{13}(x_1,x_3)$, and $\Delta g^{(3)}_{123}(x_1,x_2,x_3)$) and two background terms (1 and $\Delta g^{(2)}_{23}(x_2,x_3)$) for the vis-

ibility of the third-order double-slit interference. The maximum contribution value of $\Delta g^{(3)}_{123}(x_1,x_2,x_3)$ is about 2, while it is about 1 for both $\Delta g^{(2)}_{12}(x_1,x_2)$ and $\Delta g^{(2)}_{13}(x_1,x_3)$, and they satisfy $\Delta g^{(3)}_{123}(x_1,x_2,x_3) = \Delta g^{(2)}_{12}(x_1,x_2) + \Delta g^{(2)}_{13}(x_1,x_3)$, which agrees well with the previous conclusion that the contribution of the third-order correlation is the sum of all contributions from the second-order correlation.[18,27] It can be seen that the background term is composed of 1 and $\Delta g^{(2)}_{23}(x_2,x_3)$, and its value is about 2 as well. Thus, the contrast is the ratio of $g^{(3)}_3(x_2,x_2)$ to the background terms and is equal to $6:2$, which corresponds to the visibility of $1/2$. If the contribution of the third-order correlation term is ignored, the contrast will be $4:2$ and the visibility will be $1/3$, which is the same as the second-order case. Therefore, it can be concluded that the enhanced visibility in the thermal third-order intensity correlation measurement is due to the contribution of the third-order correlation term. For the higher-order case, one can obtain a similar conclusion. For the case of $x_3 = -x_2$, there are four contribution terms and only one background term, as shown in Fig. 5(b). Here $\Delta g^{(2)}_{23}(x_2,x_3)$ has become the contribution term. Thus, in this case the contrast is $6:1$ and the visibility is $5/7$. It is just the contribution of this term that makes the visibility in the latter case become higher. However, although the visibility has been improved, the interference pattern in the latter case has been distorted compared to the former case, as discussed in the above thermal double-slit experiments. Therefore, if one wants to achieve an *N*th-order interference pattern or ghost image in the *N*th-order intensity correlation measurements, the condition of the synchronous detection of the same light field by each reference detector must be satisfied. For the third-order ghost image experiment, if the third-order ghost imaging is performed by scanning the reference detectors in the opposite directions and CCD_1 works as the bucket detector, it can be imagined according to Eq. (2) that the third-order ghost image may be distorted or vague, and even no third-order ghost image can be obtained but instead of the superposition of two second-order ghost images.

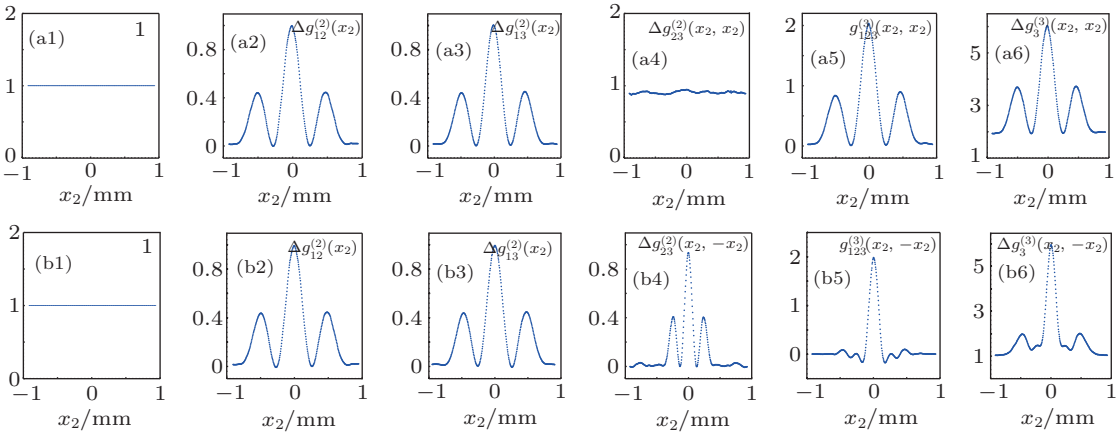


Fig. 5. (color online) Experimental plots of each term of Eq. (2) in the thermal third-order double-slit interference scheme. (a) $x_3 = x_2$ when keeping $x_1 = 0$; (b) $x_3 = -x_2$ when keeping $x_1 = 0$.

4. Conclusion

We have experimentally realized the third-order HBT measurements and double-slit interferences with pseudo-thermal light in the high-intensity limit by recording the intensities in single, double, and triple optical paths, respectively. We proved in experiment that the indispensable condition for achieving an *N*th-order interference pattern or ghost image in the *N*th-order intensity correlation measurements is the synchronous detection of the same light field by reference detectors, no matter in one, two, or even *N* detectors scheme. It is found that though the visibility and resolution of the third-order spatial HBT-type correlation function of thermal light can be enhanced when the reference detectors are scanned in the opposite directions compared with that scanned in the same direction, it does not have any effect on the higher-order interference and ghost imaging. This is because this kind of correlation only occurs within the transverse coherence area near the zero point, which distorts the interference pattern and ghost image, while the ordinary HBT-type correlation can appear at any position of the coordinate system. Moreover, we also proved the equivalence between the one detector scheme and *N* detectors scheme in thermal high-order interference and ghost imaging, that is, the interference fringes of the third-order correlation functions are almost the same, no matter whether the intensities are recorded with one detector, two detectors, or ever *N* detectors. Our experimental results are in good agreement with the theoretical prediction and have a great guiding role in the practical applications of higher-order interference and ghost imaging.

References

[1] Hanbury Brown R and Twiss R Q 1956 *Nature* **177** 27
[2] Hanbury Brown R and Twiss R Q 1956 *Nature* **178** 1046
[3] Strekalov D V, Sergienko A V, Klyshko D N and Shih Y H 1995 *Phys. Rev. Lett.* **74** 3600
[4] Gatti A, Brambilla E, Bache M and Lugiato L A 2004 *Phys. Rev. Lett.* **93** 093602
[5] Cheng J and Han S S 2004 *Phys. Rev. Lett.* **92** 093903
[6] Ferri F, Magatti D, Gatti A, Bache M, Brambilla E and Lugiato L A 2005 *Phys. Rev. Lett.* **94** 183602
[7] Cai Y J and Zhu S Y 2005 *Phys. Rev. E* **71** 056607
[8] Cao D Z and Wang K G 2005 *Phys. Rev. A* **71** 013801
[9] Xiong J, Cao D Z, Huang F, Li H G, Sun X J and Wang K G 2005 *Phys. Rev. Lett.* **94** 173601
[10] Valencia A, Scarcelli G, D'Angelo M and Shih Y 2005 *Phys. Rev. Lett.* **94** 063601
[11] Zhang D, Zhai Y H, Wu L A and Chen X H 2005 *Opt. Lett.* **30** 2354
[12] Zhai Y H, Chen X H, Zhang D and Wu L A 2005 *Phys. Rev. A* **72** 043805
[13] Zhai Y H, Chen X H and Wu L A 2006 *Phys. Rev. A* **74** 053807
[14] Scarcelli G, Berardi V and Shih Y H 2006 *Appl. Phys. Lett.* **88** 061106
[15] Scarcelli G, Berardi V and Shih Y H 2006 *Phys. Rev. Lett.* **96** 063602
[16] Shapiro J H 2008 *Phys. Rev. A* **78** 061802
[17] Chen X H, Liu Q, Luo K H and Wu L A 2009 *Opt. Lett.* **34** 695
[18] Liu Q, Chen X H, Luo K H, Wu W and Wu L A 2009 *Phys. Rev. A* **79** 053844
[19] Liu Q, Luo K H, Chen X H and Wu L A 2010 *Chin. Phys. B* **19** 094211
[20] Agafonov I N, Chekhova M V, Iskhakov T Sh and Penin A N 2008 *Phys. Rev. A* **77** 053801
[21] Agafonov I N, Chekhova M V, Iskhakov T Sh and Wu L A 2009 *J. Mod. Opt.* **56** 422
[22] Cao D Z, Xiong J, Zhang S H, Lin L F, Gao L and Wang K G 2008 *Appl. Phys. Lett.* **92** 201102
[23] Richter T 1990 *Phys. Rev. A* **42** 1817
[24] Richter T 1991 *Quant. Opt.* **3** 115
[25] Li H G, Zhang Y T, Cao D Z, Xiong J and Wang K G 2008 *Chin. Phys. B* **17** 4510
[26] Chen X H, Agafonov I N, Luo K H, Liu Q, Xian R, Chekhova M V and Wu L A 2010 *Opt. Lett.* **35** 1166
[27] Chen X H, Chen W, Meng S Y, Wu W, Wu L A and Zhai G J 2013 *J. Opt. Soc. A* **30** 1422
[28] Chan K W C, O'Sullivan M N and Boyd R W 2009 *Opt. Lett.* **34** 3343
[29] Cao B and Zhang C X 2010 *Opt. Lett.* **35** 2091
[30] Liu J B and Shih Y H 2009 *Phys. Rev. A* **79** 023819
[31] Li H, Chen Z P, Xiong J and Zeng G H 2012 *Opt. Express* **20** 2956
[32] Li H, Shi J H, Chen Z P and Zeng G H 2012 *J. Opt. Soc. A* **29** 2256
[33] Zhou Y, Simon J, Liu J B and Shih Y H 2010 *Phys. Rev. A* **81** 043831
[34] Zhou Y, Liu J B, Simon J and Shih Y H 2012 *J.Opt. Soc. B* **29** 377
[35] Bai Y F and Han S S 2007 *Phys. Rev. A* **76** 043828
[36] Ou L H and Kuang L M 2007 *J. Phys. B* **40** 1833
[37] Mandel L and Wolf E 1995 *Optical Coherence and Quantum Optics* (Cambridge: Cambridge University Press)